CHEMISTRY
A European Journal

Supporting Information

Dynamic Magnetic and Optical Insight into a High Performance Pentagonal Bipyramidal Dy^{III} Single-Ion Magnet

Yan-Cong Chen,[a] Jun-Liang Liu,*[a] Yanhua Lan,[b] Zhi-Qiang Zhong,[c] Akseli Mansikkamäki,[d, e] Liviu Ungur,[d, f] Quan-Wen Li,[a] Jian-Hua Jia,[a] Liviu F. Chibotaru,[d] Jun-Bo Han,[c] Wolfgang Wernsdorfer,[b] Xiao-Ming Chen,[a] and Ming-Liang Tong*[a]

chem_201606029_sm_miscellaneous_information.pdf

Supplementary Information

Dynamic Magnetic and Optical Insight into a High Performance Pentagonal Bipyramidal Dy(III) Single-Ion Magnet

Yan-Cong Chen,[a] Jun-Liang Liu,*[a] Yanhua Lan,[b] Zhi-Qiang Zhong,[c] Akseli Mansikkamäki,[d,e] Liviu Ungur,[d,f] Quan-Wen Li,[a] Jian-Hua Jia,[a] Liviu F. Chibotaru,[d] Jun-Bo Han,[c] Wolfgang Wernsdorfer, [b] Xiao-Ming Chen,[a] and Ming-Liang Tong*[a]

Contents

1. Computational Details

The geometry of **1** was extracted from the crystal structure. Hydrogen positions were optimized at DFT level while the coordinates of the heavier elements were kept fixed. The DFT calculations were conducted using the ORCA program suite version 3.0.3[1] using the pure BP86 GGA functional.[2-3] Scalar relativistic effects were included using the standard second order DKH Hamiltonian[4-5] in conjunction with relativistic SARC-DKH-SVP basis[6] for the Dy ion and DKH-SVP basis[7] for the other atoms.

All multiconfigurational ab initio calculations were of the CASSCF/RASSI/SINGLE_ANISO or CASSCF/XMS-CASPT2/RASSI/SINGLE_ANISO type and were performed with the MOLCAS program.[8] The development version 8.1 was used for XMS-CASPT2 calculations and the standard release version 8.0 for other calculations. All atoms were described by ANO-RCC relativistic basis sets.[9-11] A quadruple-ζ basis with polarization functions (VQZP) was used for the Dy ion, a triple-ζ basis with polarization functions (VTZP) was used for all O and Br atoms as well as the H atoms in the coordinated water molecules and a double-ζ basis with polarization functions (VDZP) was used for all other atoms.

The CASSCF calculations correlated the nine unpaired electrons occupying the seven 4f orbitals. All sextet, quartet and doublet states were optimized in state-averaged calculations for each respective multiplicity. Scalar relativistic effects were included into the CASSCF calculations using the scalar version of the exact two-component (X2C) Hamiltonian.[12] All spin sextets, 128 lowest spin quartets and 130 spin doublet states (corresponding to an energy cut-off of 50,000 cm^{-1}) were mixed by spin-orbit coupling using the restricted active space state interaction (RASSI) approach.[13] The local magnetic properties (**g**-tensors of the ground and excited Kramers doublets, crystal field parameters of the ground multiplet and transition magnetic moment matrix elements) were calculated with the SINGLE_ANISO program.[14]

The large size of the system made XMS-CASPT2 calculations on the full system prohibitively expensive and therefore the effects of dynamic correlation were calculated as a correction to the crystal field potential. First, a CASSCF calculation was conducted on the full structure and then a CASSCF and XMS-CASPT2 calculations were performed on a truncated (reduced) geometry were the phenyl and cyclohexyl groups were replaced with methyls. The ab initio crystal field parameters up to rank 12 were extracted from all three calculations. A dynamic correlation correction to the crystal field was calculated as the difference between the crystal field potentials calculated at XMS-CASPT2 level and at CASSCF level on the truncated geometry. The full corrected crystal field Hamiltonian was then constructed as a sum of the crystal field potential extracted from the CASSCF calculation on the full geometry and the dynamic correlation correction:

$$\hat{H} = \hat{V}^{\text{full}}_{\text{CASSCF}} + \left(\hat{V}^{\text{truncated}}_{\text{XMS-CASPT2}} - \hat{V}^{\text{truncated}}_{\text{CASSCF}}\right)$$

This Hamiltonian was diagonalized to obtain the final corrected energy spectrum.

2. Crystal Data and Structures

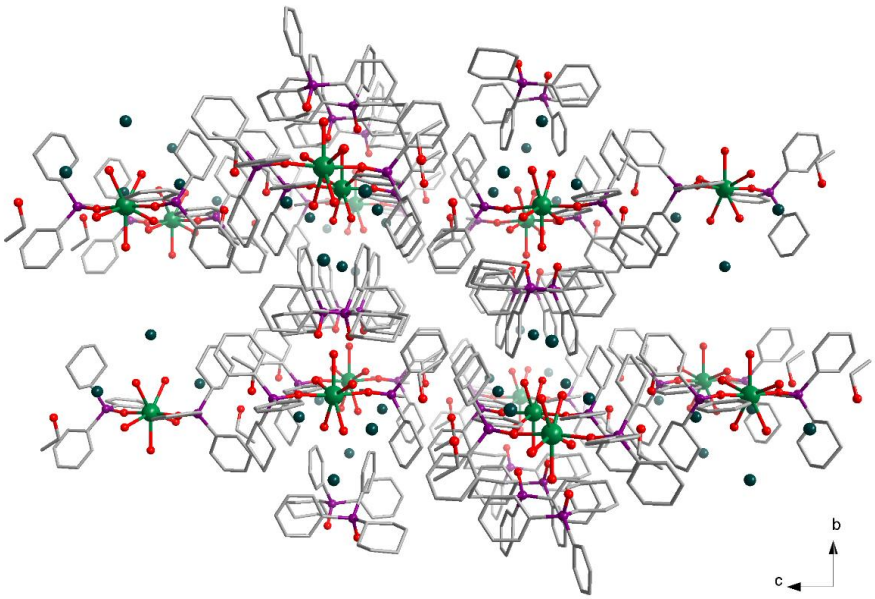

Figure S1 Crystal Structure of 1 viewed along the *a* axis. H atoms are omitted for clarity. Color Codes: Dy, green; P, purple; Br, cyan; O, red; C, gray.

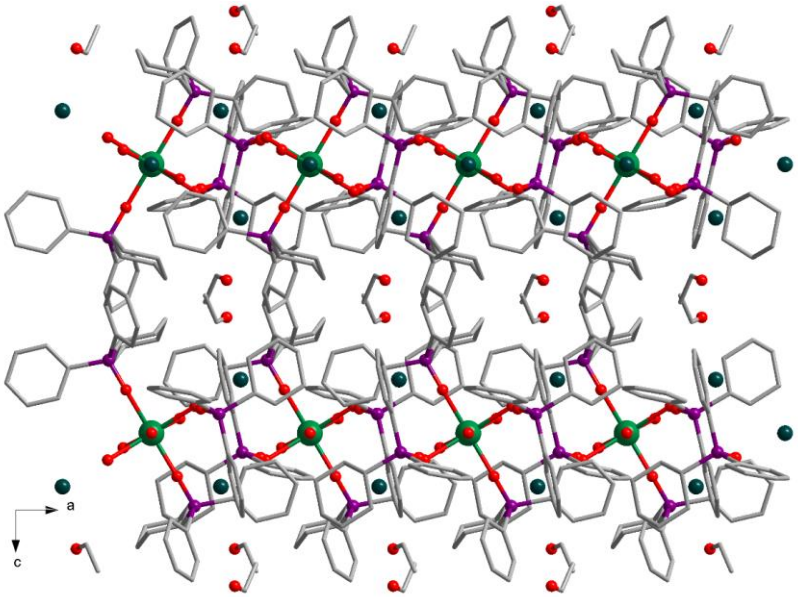

Figure S2 Crystal Structure of 1 viewed along the *b* axis. H atoms are omitted for clarity. Color Codes: Dy, green; P, purple; Br, cyan; O, red; C, gray.

Table S1 | Selected bond lengths (Å) and bond angles for **1** and **1@Y**.[a]

Bond	1	1@Y	Bond angle	1	1@Y
Dy–O1	2.217(3)	2.217(6)	O1–Dy–O1A	174.2(2)	173.8(4)
Dy–O1A	2.217(3)	2.217(6)			
Dy–O1W	2.336(5)	2.312(8)	O1W–Dy–O2W	71.69(10)	71.99(17)
Dy–O2W	2.361(4)	2.374(7)	O2W–Dy–O3W	72.12(14)	72.2(2)
Dy–O2WA	2.361(4)	2.374(7)	O3W–Dy–O3WA	72.6(2)	71.8(4)
Dy–O3W	2.380(4)	2.328(7)	O3WA–Dy–O2WA	72.12(14)	72.2(2)
Dy–O3WA	2.380(4)	2.328(7)	O2WA–Dy–O1W	71.69(10)	71.99(17)

[a]Symmetry code (A): 1-x, y, 0.5-z.

Table S2 Continuous Shape Measures calculations (CShM) for **1** and **1@Y**.[a]

Complex	HP-7 (D_{7h})	HPY-7 (C_{6v})	PBPY-7 (D_{5h})	COC-7 (C_{3v})	CTPR-7 (C_{2v})	JPBPY-7 (D_{5h})	JETPY-7 (C_{3v})
1	34.577	25.058	0.174	7.448	5.567	2.707	24.474
1@Y	34.355	24.925	0.183	7.212	5.3	2.851	24.199

HP-7 = Heptagon; HPY-7 = Hexagonal pyramid; PBPY-7 = Pentagonal bipyramid; COC-7 = Capped octahedron; CTPR-7 = Capped trigonal prism; JPBPY-7 = Johnson pentagonal bipyramid J13; JETPY-7 = Johnson elongated triangular pyramid J7.

[a] (a) Alvarez, S.; Alemany, P.; Casanova, D.; Cirera, J.; Llunell, M.; Avnir, D. *Coord. Chem. Rev*., **2005**, *249*, 1693-1708; (b) Casanova, D.; Llunell, M.; Alemany, P.; Alvarez, S. *Chem. Eur. J*., **2005**, *11*, 1479-1494.

Table S3 Crystal Data and Structural Refinements for **1** and **1@Y**.

Complex	1	1@Y
Chemical formula	$C_{76}H_{106}Br_3DyO_{11}P_4$	$C_{76}H_{106}Br_3Dy_{0.05}O_{11}P_4Y_{0.95}$
Formula Mass	1721.72	1651.81
Crystal system	Orthorhombic	Orthorhombic
a /Å	13.9130(7)	13.9262(14)
b/Å	24.5896(15)	24.547(2)
c/Å	23.6935(10)	23.679(2)
Unit cell volume/Å^3	8105.9(7)	8094.6(14)
Temperature/K	150(2)	150(2)
Space group	$C222_1$	$C222_1$
No. of formula units per unit cell, *Z*	4	4
Radiation type	$Mo_{K\alpha}$	$Mo_{K\alpha}$
Absorption coefficient, μ/mm^{-1}	2.533	2.344
No. of reflections measured	16704	22763
No. of independent reflections	8307	7922
R_{int}	0.0639	0.1383
R_1 [a] ($I > 2\sigma(I)$)	0.0482	0.0777
wR_2 [b] (all data)	0.1176	0.2485
Goodness of fit on F^2	1.055	1.026

[a]$R_1 = \Sigma||F_o| - |F_c||/\Sigma|F_o|$

[b]$wR_2 = [\Sigma w(F_o^2-F_c^2)^2/\Sigma w(F_o^2)^2]^{1/2}$.

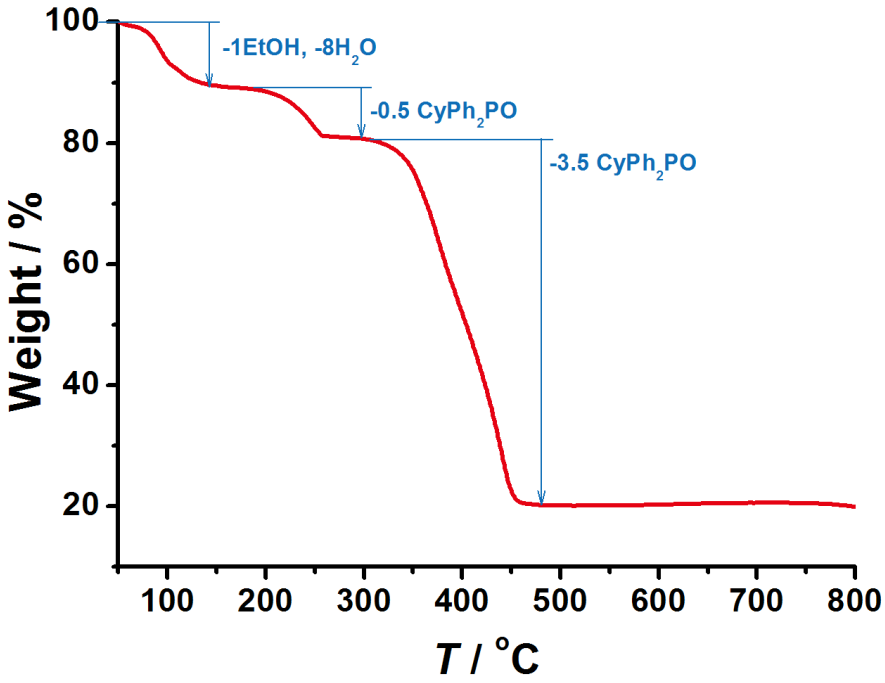

Figure S3 Thermogravimetric analysis (TGA) of 1 under N_2 atmosphere.

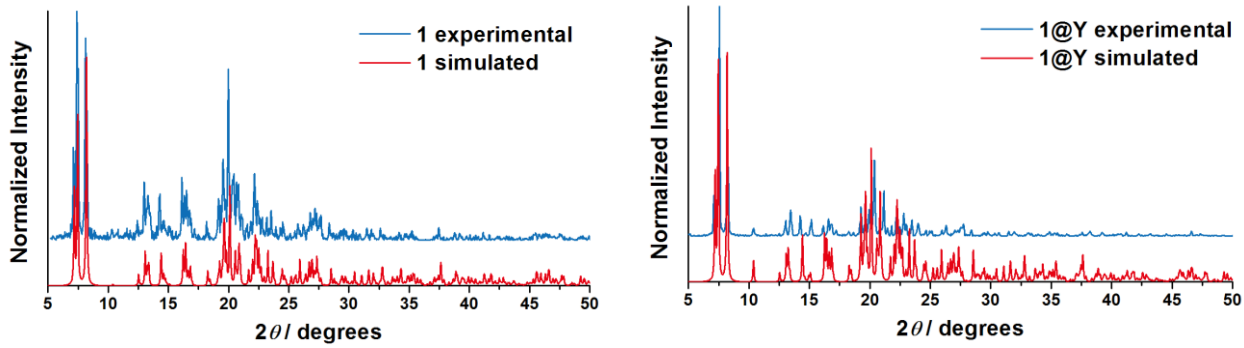

Figure S4 PXRD patterns of 1 (left) and 1@Y (right) compared with the simulated pattern from the single crystal structure.

3. Magnetic Characterization

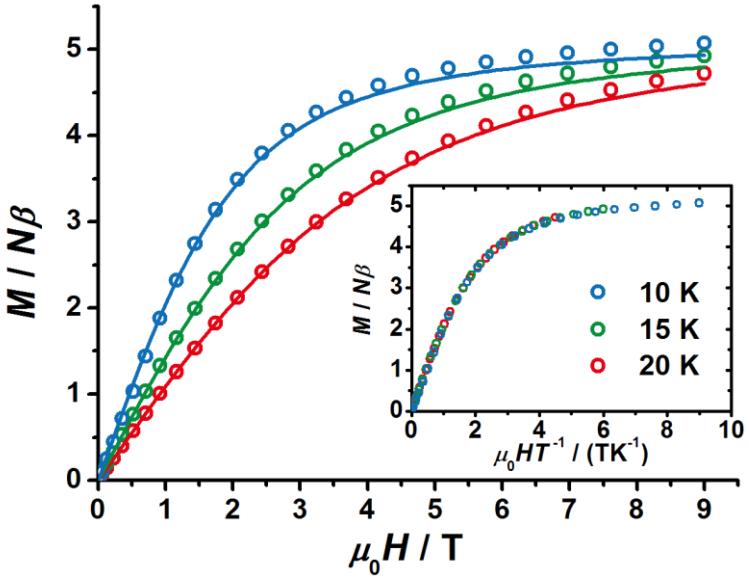

Figure S5 Variable-field magnetization data for 1 collected from 0 T to 9 T in steady fields plotted in *M* vs *H* and *M* vs *H*/*T* (inset). In even lower temperatures slow relaxation of magnetization was observed and resulted in hysteresis. The solid lines correspond to the *ab initio* calculations.

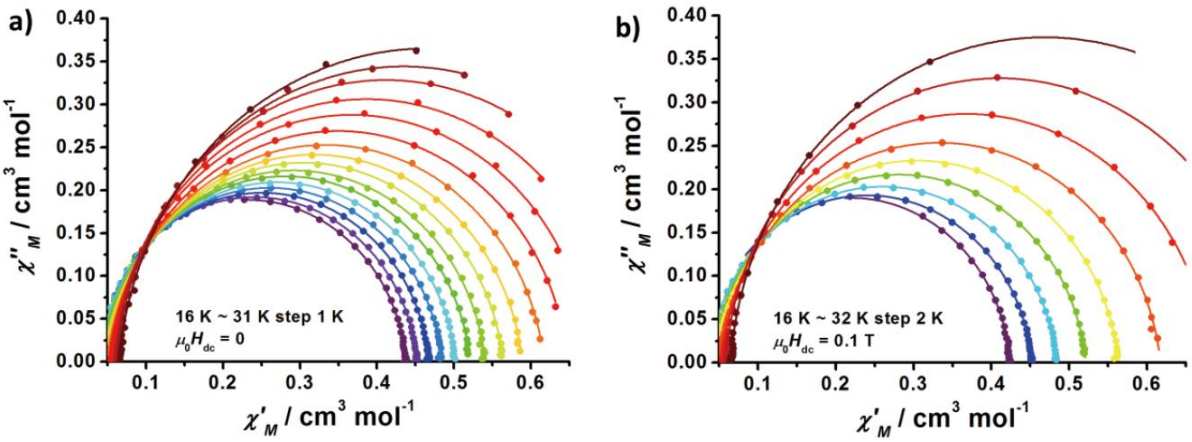

Figure S6 Cole-Cole plots for the ac susceptibilities in zero dc field (a) and a 0.1 T dc field (b) for 1. The ac susceptibilities can be nicely fitted with a generalized Debye model (solid lines) with narrow distributions indicated by the small coefficients α = 0.045~0.074 (16~31 K) for zero dc field and α = 0.034~0.073 (16~32 K) a 0.1 T dc field.

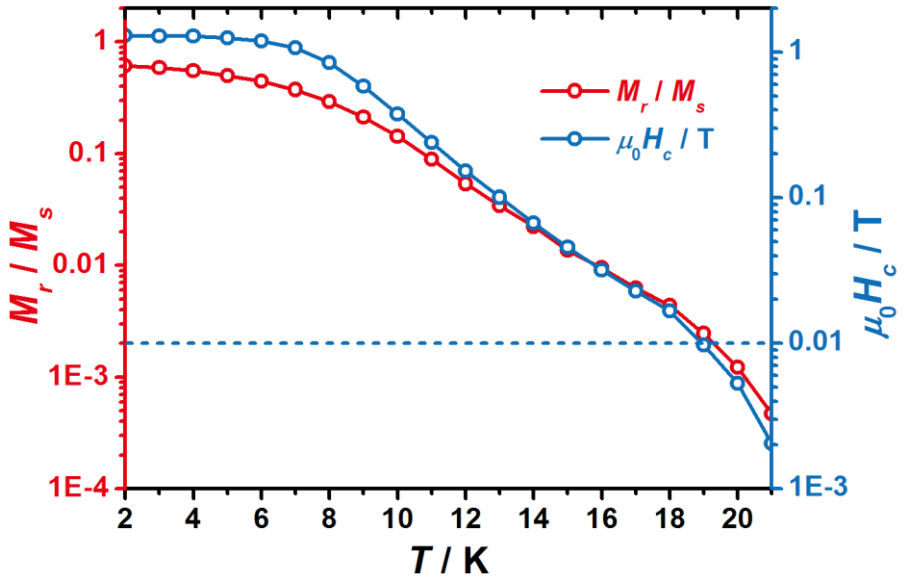

Figure S7 Temperature dependence of the normalized remnant magnetization (M_r, red) and coercive field (H_c, blue) for 1. The magnetizations are normalized to the saturated magnetization (M_s) and the dashed line corresponds to $\mu_0 H_c$ = 0.01 T. Lines are guides to the eyes.

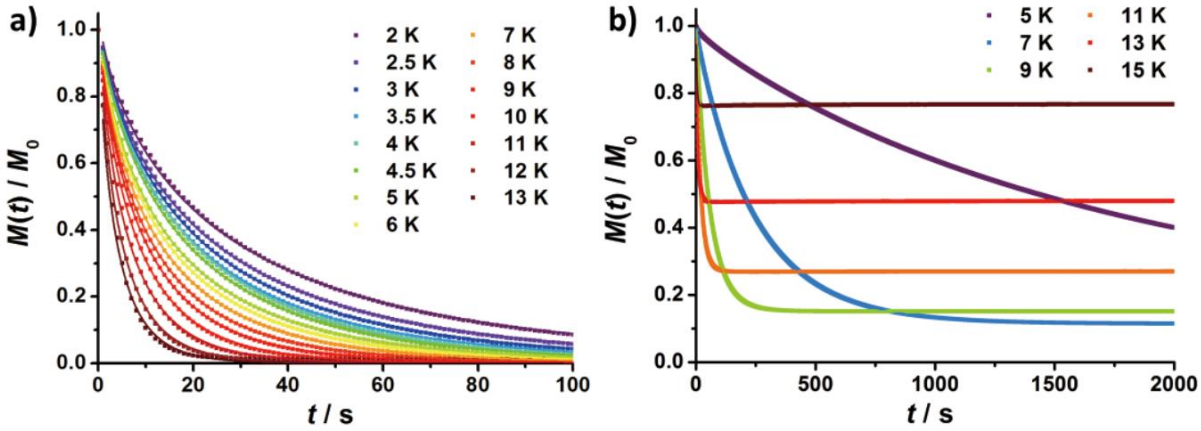

Figure S8 DC relaxation of 1 with the final field of 0 Oe (a) and 1 kOe (b). The magnetizations are plotted as normalized to M_0 (the starting value at t = 0) for clarity. The solid lines are the best fit to the exponential decay as $M(t) = M_f + (M_0 - M_f) \exp[(-t/\tau)^{\beta}]$, where τ is the relaxation time.

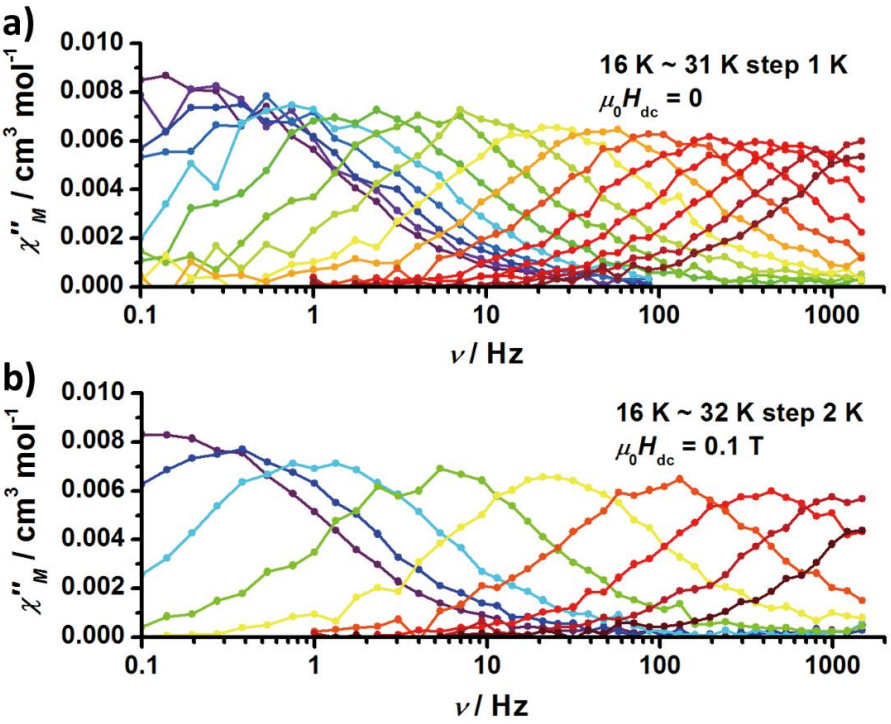

Figure S9 Frequency dependence of the out-of-phase χ''_M in zero dc field (a) and 0.1 T dc field (b) for 1@Y. Lines are guides to the eyes.

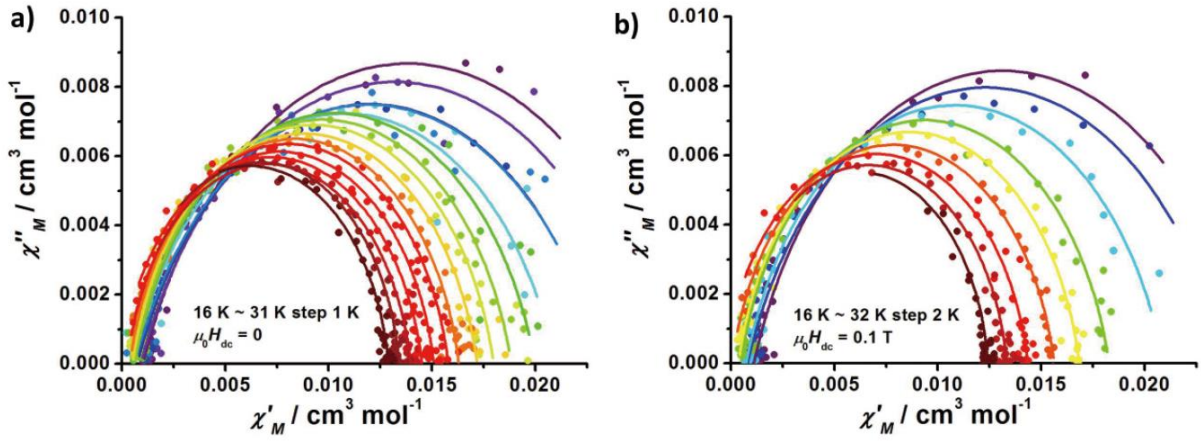

Figure S10 Cole-Cole plots for the ac susceptibilities in zero dc field (a) and a 0.1 T dc field(b) for 1@Y.

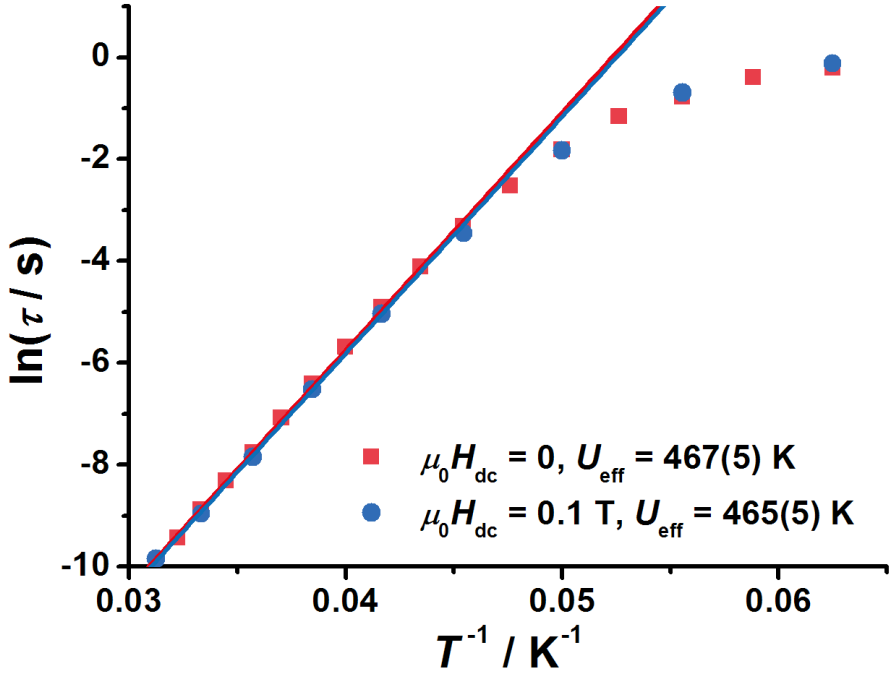

Figure S11 Temperature dependence of the relaxation time τ in zero dc field (red) and a 0.1 T dc field (blue) for 1@Y. The solid lines are the best fits to the Arrhenius law.

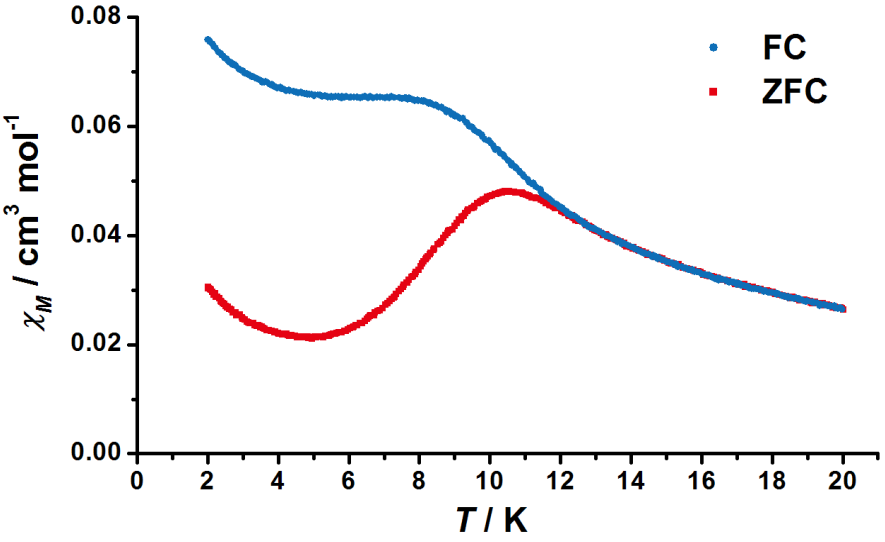

Figure S12 Zero-field-cooled / field-cooled (ZFC-FC) magnetic susceptibilities (inset) for 1@Y under a 0.1 T dc field sweeping at 2 K/min in warming mode.

4. Fluorescence Spectra

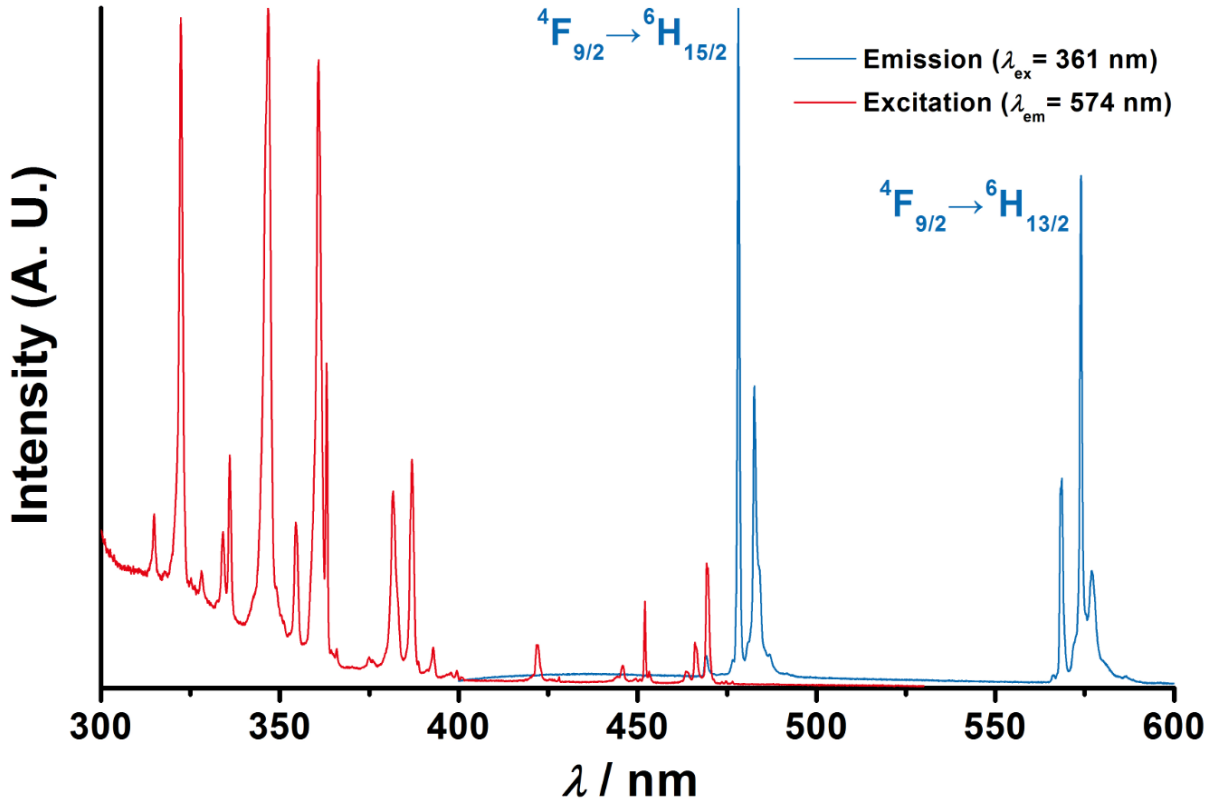

Figure S13 Fluorescence Spectra for 1 at 10 K.

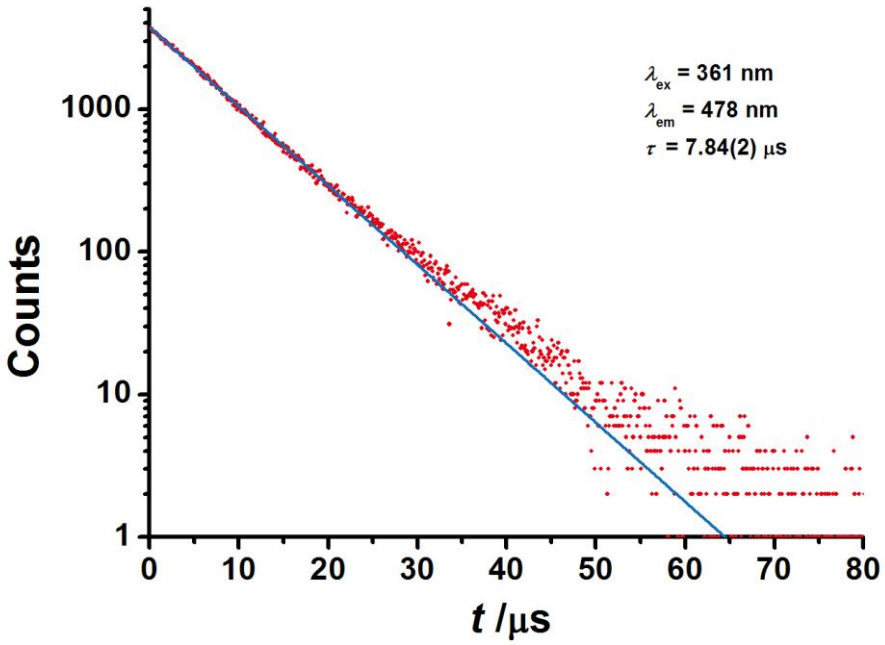

Figure S14 Fluorescence Lifetime for 1 at 10 K. The solid line is the best fit.

5. Ab Initio Calculations

Table S4 | Calculated energies (in cm^{-1} units) of the eight lowest Kramers doublets arising from the crystal field splitting of the $^6H_{15/2}$ manifold

KD	Full geometry	Truncated geometry[a]		Crystal field corrected[b]
	CASSCF	CASSCF	XMS-CASPT2	
1	0	0	0	0
2	206	130	223	297
3	242	180	284	314
4	267	214	288	370
5	342	250	371	460
6	389	321	451	507
7	425	338	467	555
8	454	365	506	588

[a] A geometry where the phenyl and cyclohexyl groups have been replaced with methyl groups. [b] Calculated by diagonalizing a crystal field Hamiltonian obtained as a sum of the ab initio crystal field potential from a CASSCF calculation on the full geometry and a dynamic electron correlation correction potential obtained as the difference in the ab initio crystal field potentials of a CASSCF and an XMS-CASPT2 calculations on a truncated geometry.

Table S5 | Percentage composition of the lowest multiplet $J = 15/2$.

	KD1		KD2		KD3		KD4		KD5		KD6		KD7		KD8	
|-15/2>	99.986	0.000	0.000	0.001	0.000	0.000	0.000	0.003	0.001	0.000	0.003	0.000	0.000	0.000	0.006	0.000
|-13/2>	0.000	0.000	0.847	0.008	76.018	22.738	0.150	0.065	0.004	0.001	0.001	0.000	0.009	0.000	0.160	0.000
|-11/2>	0.004	0.000	0.001	0.070	0.003	0.000	0.000	0.011	0.036	0.005	84.335	0.038	12.435	1.972	1.076	0.014
|-9/2>	0.005	0.000	0.018	0.001	0.094	0.025	0.168	0.000	2.258	0.141	0.011	0.012	4.192	2.141	90.911	0.024
|-7/2>	0.000	0.000	0.002	0.009	0.049	0.004	0.001	1.843	0.289	0.307	15.129	0.010	66.868	10.829	4.471	0.187
|-5/2>	0.000	0.000	1.717	0.028	0.002	0.000	2.756	0.182	85.247	6.848	0.005	0.065	0.003	0.248	2.890	0.008
|-3/2>	0.004	0.000	0.242	11.393	0.287	0.230	0.475	84.037	0.532	1.082	0.251	0.000	1.018	0.261	0.115	0.073
|-1/2>	0.000	0.000	85.340	0.324	0.479	0.071	10.308	0.002	2.975	0.275	0.000	0.139	0.005	0.019	0.063	0.001
|1/2>	0.000	0.000	0.324	85.340	0.071	0.479	0.002	10.308	0.275	2.975	0.139	0.000	0.019	0.005	0.001	0.063
|3/2>	0.000	0.004	11.393	0.242	0.230	0.287	84.037	0.475	1.082	0.532	0.000	0.251	0.261	1.018	0.073	0.115
|5/2>	0.000	0.000	0.028	1.717	0.000	0.002	0.182	2.756	6.848	85.247	0.065	0.005	0.248	0.003	0.008	2.890
|7/2>	0.000	0.000	0.009	0.002	0.004	0.049	1.843	0.001	0.307	0.289	0.010	15.129	10.829	66.868	0.187	4.471
|9/2>	0.000	0.005	0.001	0.018	0.025	0.094	0.000	0.168	0.141	2.258	0.012	0.011	2.141	4.192	0.024	90.911
|11/2>	0.000	0.004	0.070	0.001	0.000	0.003	0.011	0.000	0.005	0.036	0.038	84.335	1.972	12.435	0.014	1.076
|13/2>	0.000	0.000	0.008	0.847	22.738	76.018	0.065	0.150	0.001	0.004	0.000	0.001	0.000	0.009	0.000	0.160
|15/2>	0.000	99.986	0.001	0.000	0.000	0.000	0.003	0.000	0.000	0.001	0.000	0.003	0.000	0.000	0.000	0.006

6. References

1 Neese, F. The ORCA program system. *WIREs Comput. Mol. Sci.* **2**, 73–78 (2012).

2 Becke, A. D. Density-functional exchange-energy approximation with correct asymptotic behavior. *Phys. Rev. A.* **38**, 3098–3100 (1988).

3 Perdew, J. P. Density-functional approximation for the correlation energy of the inhomogeneous electron gas. Phys. Rev. B. 33, 8822–8824 (1986).

4 Douglas, M. & Kroll, N. M. Quantum electrodynamical corrections to the fine structure of helium. *Ann. Phys.* **82**, 89–155 (1974).

5 Hess, B. A. Relativistic electronic-structure calculations employing a two-component no-pair formalism with external-field projection operators. *Phys. Rev. A.* **33**, 3742–3748 (1986).

6 Pantazis, D. A. & Neese, F. All-electron scalar relativistic basis sets for the lanthanides. *J. Chem. Theory Comput.* **5**, 2229–2238 (2009).

7 Pantazis, D. A., Chen, X.-Y., Landis, C. R. & Neese, F. All-electron scalar relativistc basis sets for third-row transition metal atoms. *J. Chem. Theory Comput.* **4**, 908–919 (2008).

8 Aquilante, F. *et al.* Molcas 8: New capabilities for multiconfigurational quantum chemical calculations across the periodic table. *J. Comp. Chem.* **36**, 2328–2343 (2015).

9 Widmark, P.-O., Malmqvist, P.-Å. & Roos, B. O. Density matrix averaged atomic natural orbital (ANO) basis sets for correlated molecular wave functions. *Theor. Chim. Acta.* **77**, 291–306 (1990).

10 Roos, B. O., Lindh, R., Malmqvist, P.-Å., Veryazov, V. & Widmark, P.-O. Main group atoms and dimers studied with a new relativistic ANO basis set. *J. Phys. Chem. A.* **108**, 2851–2858 (2004).

11 Roos, B. O., Lindh, R., Malmqvist, P.-Å., Veryazov, V. & Widmark, P.-O. New relativistic atomic natural orbital basis sets for lanthanide atoms with applications to the Ce diatom and LuF3. *J. Phys. Chem. A.* **112**, 11431–11435 (2008)

12 Kutzelnigg, W. & Liu, W. Quasirelativistic theory equivalent to fully relativistic theory. *J. Chem. Phys.* **123**, 241102 (2005).

13 Malmqvist, P. Å., Roos, B. O. & Schimmelpfenning, B. The restricted active space (RAS) state interaction approach with spin-orbit coupling. *Chem. Phys. Lett.* **357**, 230–240 (2002).

14 Chibotaru, L. F. & L. Ungur. Ab initio calculation of anisotropic magnetic properties of complexes. I. Unique definition of pseudospin Hamiltonians and their derivation. *J. Chem. Phys.* **137**, 064112 (2012).